Supplementary Materials for
“Polaron Size and Shape Effects on Oxygen Vacancy Interactions in Lanthanum Strontium Ferrite”

Tridip Das, Jason D. Nicholas,* and Yue Qi*

Chemical Engineering & Materials Science Department, Michigan State University, 428 South Shaw Lane, 2527 Engineering Building, East Lansing, MI 48824, USA

S1. DFT Calculation Details for $La_{1-x}Sr_xFeO_3$ (LSF) Structures

The plane wave based *ab initio* simulation package, VASP (Vienna *Ab initio* Simulation Package) was used for all the ground state (0 K, zero pressure) calculations. Projector-augmented-wave (PAW) potentials with valence configurations of $5s^2 5p^6 5d^1 6s^2$ for La, $4s^2 4p^6 5s^2$ for Sr, $3d^7 4s^1$ for Fe, and $2s^2 2p^4$ for O were used to describe the valence electrons. The generalized gradient approximation (GGA) functional along with Perdew, Burke, and Ernzerhof (PBE) parameters were used to describe the exchange-correlation potentials of the constituting elements. Fe was treated with the GGA+U method with a $U_{eff} = 3$. A detailed discussion of the Fe atom U parameter selection process is provided in Sections 2.2 and 3.1a. Spin-polarized calculations were performed and the magnetic moment on each Fe was calculated by spherical integration. The accuracy for the electronic calculations was within 1 μeV. A single point energy calculation was performed to test the convergence of the cut-off energy and *k*-points for each input lattice. It was concluded from the *k*-mesh calculations that a *k*-spacing of 0.2 $Å^{-1}$ was sufficient for the required accuracy of 1 meV/atom when the cutoff energy was set to 500 eV. Ionic relaxations were performed until the Hellmann-Feynman force on each atom reached the order of 10 meV/ Å.[1]

The ground state energy for all three oxygen-stoichiometric (i.e. $\delta = 0$) LSF compositions was calculated with six different initial structures (three crystal structures, as shown in Figure 1, multiplied with two magnetic ordering arrangements), by allowing the cell shape and atom positions to relax. Among these six input structures, the one with the minimum energy per formula unit was considered as the (ground state) crystal structure for that composition. The calculated crystal structures, lattice parameters, bond lengths, low-temperature magnetic ordering arrangements, and band gaps for stoichiometric SFO, LSF55, and LFO were benchmarked with experimental or computational studies whenever available in the literature.

S2. Calculation of the Oxygen Vacancy Formation Energy (0 K) and Oxygen Vacancy Formation Free Energy (as a Function of Temperature and Oxygen Partial Pressure)

For the defect reaction given in Equation 2, the neutral oxygen vacancy formation energy, ΔE_{vac}^{f}, was calculated from the DFT+U predicted energy of a stoichiometric lattice (δ=0), $E_{perfect}^{DFT}$, and non-stoichiometric lattice, $E_{defective}^{DFT}$ (with one oxygen vacancy), using the relationship:[1]

$$\Delta E_{vac}^{f} = E_{defective}^{DFT} - E_{perfect}^{DFT} + \frac{1}{2} E_{O_2}^{DFT} \quad [1]$$

where, $E_{O_2}^{DFT}$ is the energy of an isolated oxygen molecule.[2] A detailed discussion of the computation of $E_{O_2}^{DFT}$ is available in Das *et al.*[3] Here, ΔE_{vac}^{f} was calculated with different δ by varying the supercell size, mimicking a uniform vacancy distribution.

To facilitate direct comparison with experimentally measured δ values, the computed ΔE_{vac}^{f} was converted to an oxygen vacancy formation free energy, ΔG_{vac}^{f}, as a function of temperature (T) and oxygen partial pressure (p_{O_2}) using the relationship:[4,5]

$$\Delta G_{vac}^{f} = \Delta E_{vac}^{f} + \frac{1}{2}\left(\Delta\mu_{O_2}^{0}(T) + kT ln p_{O_2}\right) \quad [2]$$

where, $\Delta\mu_{O_2}^{0}(T)$ is the free energy of oxygen gas at a temperature T and standard state pressure (p_{O_2}= 1 bar), including the excess energy due to phonon vibration contributed by the lattice oxygen. The calculation of $\Delta\mu^{0}_{O_2}(T)$ was performed utilizing available thermodynamics data, as reported in Das *et al.*[3] Since ΔG^{f}_{vac} may increase with increasing LSF oxygen non-stoichiometry, a generalized equation to predict the oxygen vacancy site fraction, X as a function of temperature, oxygen partial pressure and vacancy concentration was utilized:

$$\frac{X}{1-X} = \exp\left(-\frac{\Delta G^{f}_{vac}(T,p,X)}{RT}\right) \qquad [3]$$

Note, this equation can be used for both dilute and interacting vacancies. The oxygen vacancy site fractions were calculated by solving Equation 6.[3]

S3. Partial Density of States (PDOS) and Band Gap Calculations for Different $La_{1-x}Sr_xFeO_3$ (LSF) Structures

Figure S1 shows the band gap for each energetically favored lattice structure. The partial density of states (PDOS) was calculated for both FM and AFMG ordering in LFO as shown in Figures 4a and 4b. The computed band gap was 0.5 and 2.0 eV for FM and AFMG ordering, respectively. The band gap predicted in AFMG LFO was comparable to the experimentally observed optical band gap of 2.1 eV measured at room temperature.[6] Cubic SFO shows a metallic behavior,[7] as correctly predicted in Figure 4e. The good match between the various predicted and measured properties for the other $SrFeO_{3-\delta}$ phases can be found in our previous study.[3] The PDOS was calculated for both FM and AFMG magnetic ordering in LSF55 and reported in Figure 4c and 4d. Though there are few DOS observed close to Fermi energy with a FM orientation (Figure 4c), the AFMG ordered structure has an energy gap of 1.6 eV, comparable to earlier computational studies.[8]

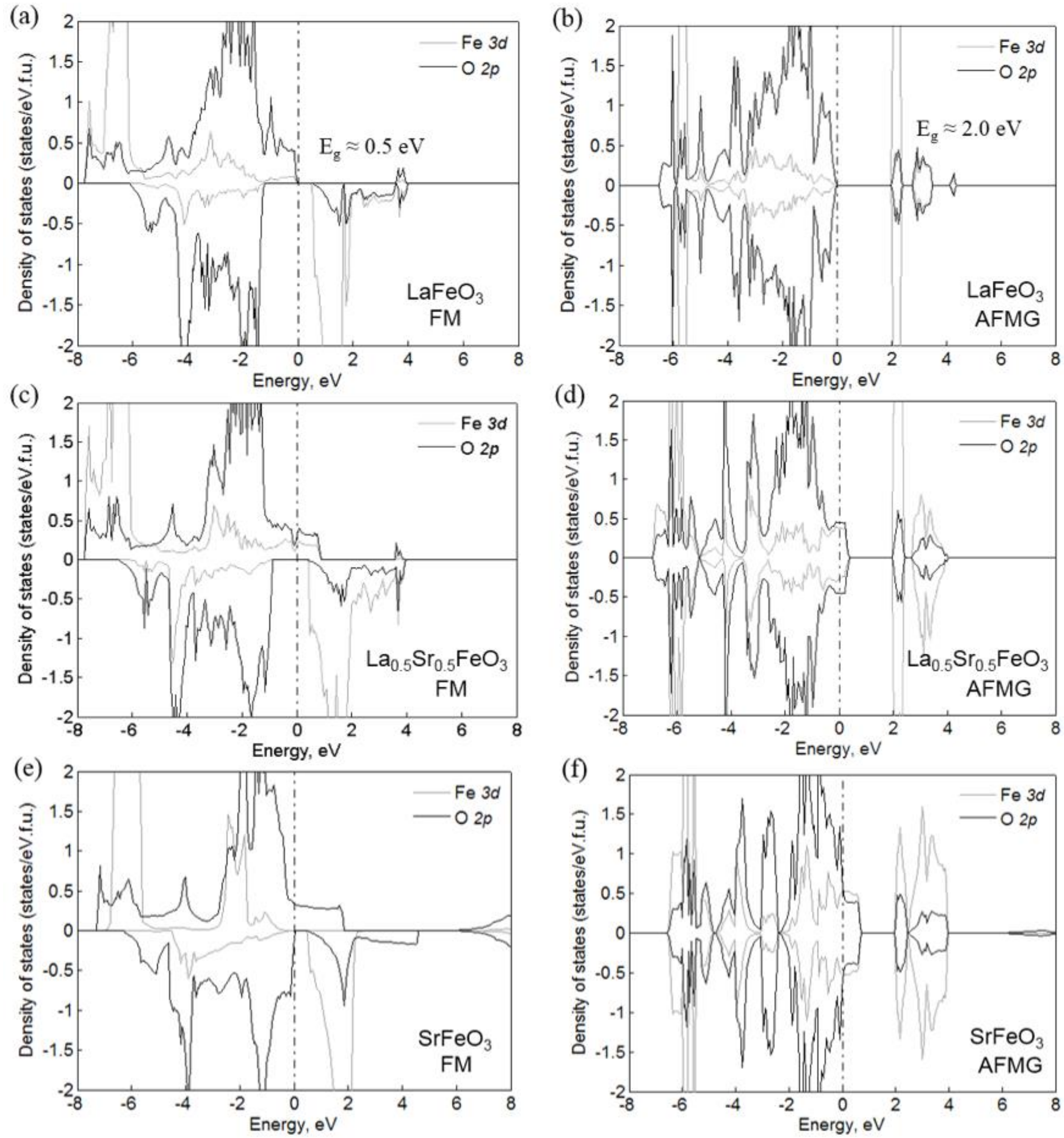

Figure S1. GGA+U (=3) partial density of states calculations for (a-b) orthorhombic LaFeO$_3$, (c-d) rhombohedral La$_{0.5}$Sr$_{0.5}$FeO$_3$, and (e-f) cubic SrFeO$_3$. The gray and black lines represent the Fe *3d* and O *2p* states respectively.

References:

(1) Lee, C.-W.; Behera, R. K.; Wachsman, E. D.; Phillpot, S. R.; Sinnott, S. B. Stoichiometry of the $LaFeO_3$ (010) Surface Determined from First-Principles and Thermodynamic Calculations. *Phys. Rev. B* **2011**, *83* (11), 115418.

(2) David Sholl; Janice A Steckel. *Density Functional Theory: A Practical Introduction*, April 2009.; WILEY, 2009.

(3) Das, T.; Nicholas, J. D.; Qi, Y. Long-Range Charge Transfer and Oxygen Vacancy Interactions in Strontium Ferrite. *J. Mater. Chem. A* **2017**, *5* (9), 4493–4506.

(4) Zhang, W.; Smith, J. R.; Wang, X.-G. Thermodynamics from Ab Initio Computations. *Phys. Rev. B* **2004**, *70* (2), 024103.

(5) Reuter, K.; Scheffler, M. Composition, Structure, and Stability of RuO2(110) as a Function of Oxygen Pressure. *Phys. Rev. B* **2001**, *65* (3), 035406.

(6) Arima, T.; Tokura, Y.; Torrance, J. B. Variation of Optical Gaps in Perovskite-Type 3d Transition-Metal Oxides. *Phys. Rev. B* **1993**, *48* (23), 17006–17009.

(7) Reehuis, M.; Ulrich, C.; Maljuk, A.; Niedermayer, C.; Ouladdiaf, B.; Hoser, A.; Hofmann, T.; Keimer, B. Neutron Diffraction Study of Spin and Charge Ordering in $SrFeO_{3-\delta}$. *Phys. Rev. B* **2012**, *85* (18), 184109.

(8) Ritzmann, A. M.; Muñoz-García, A. B.; Pavone, M.; Keith, J. A.; Carter, E. A. Ab Initio DFT+U Analysis of Oxygen Vacancy Formation and Migration in $La_{1-X}Sr_xFeO_{3-\delta}$ = 0, 0.25, 0.50). *Chem. Mater.* **2013**, *25* (15), 3011–3019.